DEPENDENCE OF TISSUE OPTICAL PROPERTIES ON SOLUTE-INDUCED CHANGES IN REFRACTIVE INDEX AND OSMOLARITY

Hanli Liu, Bertrand Beauvoit, Mika Kimura, and Britton Chance
University of Pennsylvania, School of Medicine, Johnson Research Foundation, Department of Biochemistry and Biophysics, D501 Richards Building, Philadelphia, Pennsylvania 19104

ABSTRACT

Additions of a solute/carbohydrate in tissue affect the size of tissue cells and the refractive indexes of the extra- and intracellular fluids, and thus the overall tissue scattering properties. We use both the Rayleigh-Gans and Mie theory approximation in calculating effects of the osmolarity and refractive indexes on the reduced scattering coefficient of tissue, and employ photon diffusion theory to associate the reduced scattering coefficient to the mean optical path length. The calculations show that changes of scattering in tissue depend not only on the change in extracellular refractive index but also on the change in osmolarity, and thus on the change in cell size and volume fraction. Experimentally, we have utilized time-domain and frequency-domain NIR techniques to measure the changes of optical properties caused by an addition of a solute in tissue models and in perfused rat livers. The temperature-dependent path length measurement of the perfused liver confirms the dependence of tissue scattering on the tissue cell size. The results obtained from the liver with three kinds of carbohydrate perfusion display different scattering aspects and can be well explained by changes in cell size and in extracellular as well as intracellular refractive indexes. The consistency between the theoretical and experimental results confirms the dependence of optical properties in (liver) tissue on both tissue osmolarity and relative refractive indexes between the extracellular and intracellular compartments. This study suggests that the NIR technique is a novel and useful tool for noninvasive, physiological monitoring.

Keywords solute; light scattering in tissue; Mie theory approximation; liver tissue; refractive index; osmotic stress; near infrared spectroscopy.

1 INTRODUCTION

Recently developed near-infrared spectroscopy (NIR) using time domain, frequency domain, and continuous wave techniques offers a noninvasive means to determine hemoglobin oxygenation in the brain, muscle, and other *in situ* biological organs.[1–4] On the other hand, a number of recent studies have focused on the possibility of using the same techniques to monitor a change of glucose concentration in tissue.[5,6] The basis in the latter case rests on the fact that a change of refractive index in the extracellular fluid due to the presence of additional glucose causes a small change in overall scattering property of the tissue that could be detected by the NIR techniques. Chance et al.[7] show that in lipid and yeast cell suspensions, an increase in concentration of a general solute, such as sugars and electrolytes, gives rise to a decrease of scattering factor of the suspension. These results are in good agreement with those given in Refs. 5 and 6. However, in the tissue measurement performed on a perfused rat liver, the results obtained by adding mannitol (or glucose) to the perfusate of the perfused liver were[7] in contrast to those in the lipid suspensions and cannot be well explained by the change of only refractive index.

Volume changes upon exposure to anisosmotic media have been extensively studied in a great variety of cells: hepatocytes, *in situ* or isolated from the organ, ascites tumor cells, red blood cells, astrocytes, and glioma cells. The physiological significance and the mechanisms of the volume changes have been reviewed by Haussinger and Lang.[8] The conventional response of a cell, such as a red blood cell, to anisosmotic media is an ''osmometerlike'' effect. Specifically, a hypo-osmotic stress, made by lowering the electrolyte (such as Na^+, K^+, and Cl^-) concentration in the extracellular medium, results in movement of water from extracellular to intracellular space and induces an increase of the cell volume (i.e., cell swelling). In contrast, hyperosmotic stress, made by raising the osmolarity of the extracellular medium by increasing the electrolyte or nonelectrolyte (such as carbohydrates) concentration, induces a decrease of the cell volume (i.e., cell

shrinkage). Thus, besides changing the refractive index of the extracellular fluid, additions of a solute to tissue can unbalance the nonelectrolyte concentration between the extra- and intracellular fluids and lead to possible cell shrinkage, depending on the permeability of the cell for the solute. As evidence, mannitol has been used clinically as a treatment agent to decrease intracellular water content and to decrease brain swelling in head injuries since mannitol is osmotically active, (R. L. Veach, personal communication). Consequently, the change in cell size can affect light scattering of the cells,[9] and thus can affect overall scattering behavior of the tissue. In order to employ NIR techniques for broad use in noninvasive physiological monitoring, we wish to show in this paper the dependence of tissue optical properties on solute-induced changes in refractive index as well as in osmolarity.

Many researchers have successfully utilized Mie calculations to predict scattering properties of red blood cells,[10,11] yeast suspensions,[12] and other scatterers in living tissues,[13] provided that the radius and range of refractive index of the scatterers are known. Furthermore, an approximated approach of Mie theory has been suggested by Graaff et al.,[14] showing the dependence of the reduced scattering cross section explicitly on the scatterer size, scattered light wavelength, and refractive indexes. Although Mie theory has its limitation in dealing with nonspherical particles, it does provide a first-order description of optical effects in nonspherical particles and correctly illustrates many nonobvious, small-particle effects. In addition, the Rayleigh-Gans (or Rayleigh-Debye-Gans) approximation is suitable for arbitrarily-shaped particles that are not too small, namely, particle sizes comparable to the wavelength of the scattered light.[15] It has been shown[14] that the Mie calculation and the Rayleigh-Gans approximation give consistent results with a maximum deviation of 20%.

In this paper, we employ both the Mie theory approximation and the Rayleigh-Gans approximation in calculating the effects of refractive indexes and osmolarity on reduced scattering coefficient of tissues. Also, we apply photon diffusion theory to associate the reduced scattering coefficient with the mean optical path length. Experimentally, we utilize the time- and frequency-domain NIR techniques to measure changes in optical properties due to the addition of a solute in tissue models and in perfused rat livers. Based on the theoretical calculations, we show that changes of scattering in tissue depend on changes not only in extracellular refractive index but also in intracellular refractive index as well as in cell size of the tissue. The consistency between the theoretical and experimental results clearly demonstrates that variation in cell size plays an important role in determining changes in the scattering properties of tissue.

2 THEORETICAL AND PHYSIOLOGICAL BACKGROUND

2.1 REDUCED SCATTERING COEFFICIENT AND MEAN OPTICAL PATH LENGTH

2.1.1 Approximations for the Reduced Scattering Cross Section

According to a recent study by Graaff et al.,[14] the Mie theory can be well approximated to give the following expression for the reduced scattering cross section, σ'_s,

$$\sigma'_s = \sigma_s(1-g) = 3.28\pi a^2 \left(\frac{2\pi a n_{ex}}{\lambda} \right)^{0.37} (m-1)^{2.09},$$ (1)
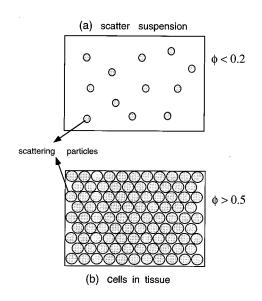
where σ_s is the scattering cross section, g is the average cosine of the scattering angle, a is the radius of the scattering particle, λ is the wavelength of the scattered light in vacuum, $m = (n_{in}/n_{ex})$ is the refractive index of the scatterers relative to the surrounding medium, and n_{in} and n_{ex} are refractive indexes of the intracellular and extracellular fluid, respectively. In the case of model or cell suspension systems, n_{in} and n_{ex} represent refractive indexes of the scattering particle and suspension solution, respectively. Three restrictions for a high accuracy of Eq. (1) are (1) the g factor must be larger than $0.9(g>0.9)$, (2) the particle radius and wavelength of the scattered light must satisfy $5<(2\pi a n_{ex}/\lambda)<50$, and (3) m must be limited in the range of $1<m<1.1$. With the use of near-infrared light, these three conditions are often satisfied in most living tissues and blood.[14] Although in some cases these conditions are not fully satisfied, Eq. (1) is still useful for estimating with a certain accuracy the dependence of tissue scattering properties on scatterer size, scattered-light wavelength, and refractive indexes of the intra- and extracellular fluid.

If Eq. (1) is not fully applicable due to the violation of the three requirements mentioned above, the Rayleigh-Gans approximation[14] provides an alternative method to obtain σ'_s:

$$\sigma'_s = \frac{9}{256\pi} \left| \frac{m^2-1}{m^2+2} \right|^2 \left(\frac{\lambda}{n_{ex}} \right)^2 \int_0^\pi (\sin u - u \cos u)^2$$

$$\times \frac{(1+\cos^2\theta)\sin\theta(1-\cos\theta)}{\sin^6\left(\frac{\theta}{2}\right)} \, d\theta,$$ (2)

where $m = n_{in}/n_{ex}$ and $u = 2(2\pi a n_{ex}/\lambda)\sin(\theta/2)$.

In comparison, Eq. (1) affords a simple and explicit solution for σ'_s, but its use is limited by certain restrictions. On the other hand, Eq. (2) can be used in a much broader range of applications since it does not have a validation requirement, but one often needs numerical integration to obtain σ'_s values when using Eq. (2). In this paper, we use both

Fig. 1 Schematic diagram illustrating the difference in volume fraction of scattering particles between a scatterer suspension (a) and tissue or blood (b). In case (a), the volume fraction of the scatterers is ϕ=0.026, whereas in case (b), the volume fraction of the scatterers is ϕ=0.73.

Eqs. (1) and (2) to obtain σ_s': the former one for fast information (estimation) and the latter one for better accuracy.

2.1.2 Reduced Scattering Coefficient

In a highly multiple-scattering medium, the reduced scattering coefficient, μ_s', is related to σ_s' by $\mu_s' = \gamma\sigma_s'$, where γ is the total number of scattering particles per unit volume, i.e., the number density.[16] γ can be given as ϕ/v_{par}, where ϕ is the volume fraction of the particles relative to the total volume, and v_{par} is the volume of a single scattering particle[13] and can be expressed as $(4/3)\pi a^3$ for a spherical scatterer. Thus, we can have

$$\mu_s' = \frac{\phi}{v_{par}}\sigma_s' = \frac{3\phi}{4\pi a^3}\sigma_s', \qquad (3)$$

where σ_s' can be substituted by Eq. (1) or (2), respectively, for the Mie theory approximation or the Rayleigh-Gans approximation. Equation (3) is valid for sufficiently small ϕ (ϕ<0.2), such as in cell or scatterer suspensions. For ϕ>0.5, which is very common for scatterers in tissue and blood, the scattering particles are densely packed, and the whole solution may be viewed as a homogeneous medium with the scattering particles made of the interparticle space. These two cases are schematically illustrated in Figs. 1(a) and 1(b), respectively. In the limit of $\phi \to 1$, the interparticle space disappears and μ_s' should approach 0. Based on this consideration, we employ the strategy developed by Ishimaru[16] and others[10,11] for red blood cells and give the following modified expression of μ_s' for biological tissues:

$$\mu_s' = \frac{3\phi(1-\phi)}{4\pi a^3}\sigma_s', \qquad (4)$$

where σ_s' is given by Eq. (1) or Eq. (2). Using the Mie theory approximation by replacing Eq. (1) into Eqs. (3) and (4), one can show that μ_s' has both a refractive index-dependent factor $n_{ex}^{0.37}[(n_{in}/n_{ex})-1]^{2.09}$ and a size-dependent factor, either $(\phi/a)(2\pi a/\lambda)^{0.37}$ for suspensions or $[\phi(1-\phi)/a](2\pi a/\lambda)^{0.37}$ for tissue. The Rayleigh-Gans approximation for μ_s' also contains a refractive index-dependent and a size-dependent factor, but they cannot be expressed as explicitly as those in the Mie theory approximation.

2.1.3 Mean Optical Pathlength

The diffusion approximation of transport theory has been widely used as the theoretical basis to describe light propagation within a highly scattering medium for a given geometry.[17,18] The solution of the time-domain diffusion equation allows us to calculate the mean optical pathlength $\langle L \rangle$ of light traveled before detection by $\langle L \rangle = c\langle t \rangle$, where c is the speed of light traveled in a mean time $\langle t \rangle$ in the scattering medium. In a semi-infinite, reflectance geometry, $\langle t \rangle$ can be given as

$$\langle t \rangle = \frac{\int R(\rho,t)t\,dt}{\int R(\rho,t)\,dt}, \qquad (5)$$

where $R(\rho,t)$ is the reflectance of impulse light detected on the medium surface at time t and at distance ρ away from the light source.[19] After substituting $R(\rho,t)$ in $\langle t \rangle$ and simplifying $\langle t \rangle$, we obtain an expression relating $\langle L \rangle$ to the absorption (μ_a) and reduced scattering (μ_s') coefficients by

$$\langle L \rangle = \frac{\sqrt{3}}{2}\rho\sqrt{\frac{\mu_s'}{\mu_a}}\left[\frac{1}{1+\frac{1}{\rho[3\mu_a\mu_s']^{1/2}}}\right]. \qquad (6)$$

So $\langle L \rangle$ can be a marker to monitor a change in absorption or scattering properties in the medium under study. Furthermore, the first-order approximation of Eq. (6) is

$$\langle L \rangle = \frac{3}{2}\rho\sqrt{\frac{\mu_s'}{\mu_a}} - \frac{1}{2\mu_a}, \qquad (7)$$

which, for a constant-absorption system, leads to

$$\Delta\langle L \rangle = \frac{\sqrt{3}}{4}\rho\frac{1}{\sqrt{\mu_a\mu_s'}}\Delta\mu_s'. \qquad (8)$$

Both Eqs. (7) and (8) indicate that an increase in scattering results in an increase in mean optical pathlength.

2.2 PHYSIOLOGICAL BACKGROUND

2.2.1 Origins of Light Scattering in Living Tissues

Previous studies[13,20] showed that light scattering of the rat liver results mainly from both the whole hepatocyte volume and the intracellular organelles, including mitochondria. Those studies suggested that mitochondria are the major source for light scattering in tissue by showing that about 85% of the reduced scattering of the liver originates from mitochondria. However, either Mie theory or the Rayleigh-Gans approximation fails to fully describe the scattering caused by the intracellular organelles. In order to employ these two approximations to take into account the scattering due to both the cells and the mitochondria, we perform the calculations in two steps. The first step is to calculate the scattering change in cellular scale, and the second is to consider the scattering change caused by mitochondria. The parameters required for the calculations are chosen correspondingly. Then, by comparing the calculations with the experimental results, we may learn what the major factors are that cause scattering change in tissue.

2.2.2 Volume Regulation of Cells and Effect of Solution Composition on Nonelectrolyte-Induced Shrinkage

Depending on the species and the tissue type, the volume change that takes place in cells upon exposure to anisosmotic media is regulated. For instance, if hepatocytes (liver cells) are suddenly exposed to a hypotonic medium, they initially swell, but within minutes they can regain nearly their original volumes. This behavior has been named regulatory cell volume decrease and is governed by the activation of K^+ and Cl^- efflux. On the other hand, if the cells are suddenly exposed to a hypertonic medium, they initially shrink, but within minutes they attain nearly their initial volumes. This behavior has been named regulatory cell volume increase and is caused by the activation of Na^+ and Cl^- influx. However, neither the regulatory volume increase nor decrease completely restores the initial cell volume, and the liver cells are left in either a slightly swollen or slightly shrunken state. In addition, the mechanisms that regulate volume at the cellular (nature of ions) and molecular level (carriers responsible for ion efflux or influx) are different from one tissue type to another one.[8]

In the liver, when hepatocytes are subjected to hypertonic stress by the addition of a carbohydrate into the extracellular medium, there is either only a partial recovery from the shrunken state or none, depending on the nature of the carbohydrate. For instance, the time course of the sorbitol-induced shrinkage does not show any regulatory volume increase.[21] In contrast, sucrose- and mannitol-induced shrinkage is followed by a partial recovery of the initial volume. These discrepancies have been explained by different permeability of the hepatocyte toward the three nonelectrolytes used in the studies. The higher the cellular permeability to the sugar, the faster the equilibration of the osmolarity between the two compartments, and the faster the recovery from the shrunken state.[22,23]

Furthermore, when the modification in extracellular osmolarity leads to cell volume changes in tissue, this may largely affect the mitochondrial compartment.[24] Similar to tissue cells, if mitochondria are under an imbalance of osmotic pressure, they will change their intramitochondrial volume,[25] which might lead to a change in light-scattering property.[26] Therefore, the dependence of scattering on changes in both cellular and intracellular (i.e., mitochondrial) volume is considered in the following calculations in this paper.

3 METHODS AND MATERIALS

In this study, we utilized time-domain and frequency-domain NIR methods for different cases of measurements to show changes in absorption and scattering properties as well as optical path length caused by the introduction of a solute in suspensions or in perfused rat livers. Time-resolved spectroscopy is considered a gold standard to measure the optical properties of a highly scattering medium; the frequency-domain method can give a transient response of mean path length change. Since these two methods have been well developed, for detailed instrumentation, we refer the reader to Ref. 27 for the time-domain method and Refs. 2 and 17 for the frequency-domain method. The wavelengths used were 830 and 816 nm for the time- and frequency-domain methods, respectively.

In the lipid or cell suspension measurements, a cylindrical container 17 cm in diameter and 10 cm in height was filled with distilled water and appropriate concentrations of a scattering medium. A commercial product, Intralipid (Kabi Pharmatica, Clayton, North Carolina) with a 20% concentration was diluted to 0.5–2.5% (vol/vol). During the measurements, 50 mM solutions of glucose and mannitol were added to the lipid or cell suspensions and titrated for changing optical properties, namely, absorption and reduced scattering coefficients (μ_a, μ_s'). The light source and detector connected to one of the NIR detection systems mentioned above was placed 3 cm either from the top of the suspension surface or on the side of the container.

In rat liver perfusion experiments, we used male Sprague-Dawley rats of 300 to 350 g and anesthetized a rat by intraperitoneal injection of pentobarbital (50 mg/kg weight). The rats were starved 24 h to normalize physiological conditions of the liver. After being removed from the rat, the liver was perfused by Krebs–Ringer buffer, which contained 2 mM glucose and was oxygenated by a mixture of 95% oxygen and 5% carbon dioxide. After the liver perfusion became stable (20 to 30 min), the perfusate was switched between the buffer and other so-

lutions containing different concentrations of carbohydrates. The light source and detector were 1.5 cm apart and attached to the major lobes of the liver.

In simulations, Eqs. (3) and (4) were used for the suspension and tissue cases, respectively, to calculate changes in reduced scattering coefficient under various conditions. In the Rayleigh-Gans approximation, numerical integration for calculating Eq. (2) was done with a total of 900 θ angles between 0 and 180 deg.
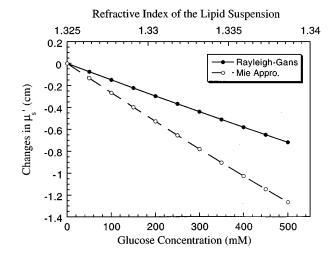
4 RESULTS

The addition of a solute to a lipid suspension will result in an increase in refractive index of the suspension but will not change the size of the lipid particles. Furthermore, it is known that exposure of living tissue, such as the perfused rat liver, to hyperosmotic stress will result in transient cellular shrinkage followed by volume-regulatory K^+ uptake.[28] However, no significant cellular shrinkage and K^+ uptake will occur in response to the hyperosmotic solution if the solute permeability of the cells is comparable to the permeability of water.[28] The introduction of a solute to a living tissue can have several effects: (1) the refractive index of the extracellular fluid can increase, while the refractive index of the intracellular fluid remains constant; (2) the tissue cells can swell or shrink due to changes in osmolarity, which drives the water movement between the extracellular and intracellular compartments; (3) the intracellular refractive index may also change as the solute is transported into the cell; this may lead to a change in volume of mitochondria, the major source of light scattering in tissue. In the following section, we describe the simulation and the experimental results based on these cases.

4.1 SIMULATIONS OF LIGHT SCATTERING FROM LIPID SUSPENSIONS, TISSUE CELLS, AND MITOCHONDRIA

4.1.1 Light Scattering in Lipid Suspensions

It is simple to calculate light scattering caused by the addition of a solute to lipid suspensions: the only variable for the calculation is the refractive index of the suspension fluid (n_{ex}), assuming that the scattering particle radius a and the refractive index of scattering particles n_{in} are not affected by the solute. To simulate the dependence of the reduced scattering coefficient μ_s', on n_{ex} for a 0.5% Intralipid–glucose suspension at 800 nm, we used the following parameters: $a = 0.25$ μm, $\lambda = 0.8$ μm, $\phi = 0.005$, $n_{in} = 1.46$, and $n_{ex} = 1.325 + 2.73 \times 10^{-5} \times [C]$, where [C] is the millimolar glucose concentration.[5] The calculated results using the two approximations are given in Fig. 2, which shows a decrease of μ_s' values with an increase in glucose concentration added (bottom scale) and a corresponding refractive index of the lipid suspension (top scale). Notice
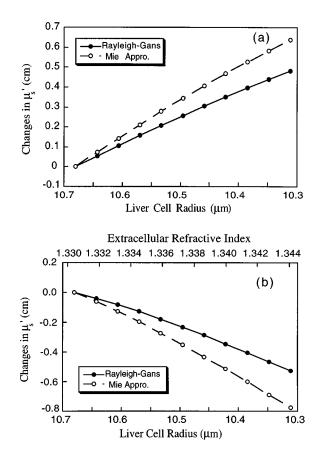

Fig. 2 Simulation results of the reduced scattering coefficient, μ_s', for a 0.5% Intralipid–glucose suspension. The calculations are based on Eq. (3) with both the Rayleigh-Gans approximation (solid circles) and Mie theory approximation (open circles). The refractive index of the lipid suspension (n_{ex}) as a function of the added glucose concentration is given in the text.

that the Mie theory approximation here is not accurately applicable since $2\pi a n_{ex}/\lambda = 2.6$, but it gives a correct trend.

4.1.2 Light Scattering by Tissue Cells

Since the cell volume fraction ϕ is usually greater than 0.5 for tissues, Eq. (4) is used in this section. Here, we consider several situations for the simulations: (1) changes in cell size only; (2) changes in refractive index of the extracellular fluid only; (3) changes both in cell size and refractive index of the extracellular fluid; and (4) changes in cell size and refractive indexes of the extra- and intracellular fluid. The fact that introducing a carbohydrate into tissue causes cell shrinkage is considered in the simulations.
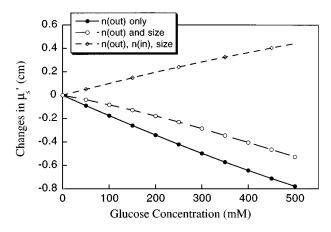
Figure 3(a) is a set of simulation results that show that changes in μ_s' depend on only the cell radius at $\lambda = 800$ nm, based on both the Rayleigh-Gans and Mie approximations. The parameters used here are based on the perfused liver with $a_0 = 10.68$ μm, $\phi_0 = 0.8$,[13] $n_{ex} = 1.33$, and $n_{in} = 1.38$,[29] where a_0 and ϕ_0 are the initial cell radius and initial cell volume fraction, respectively. In this calculation, n_{ex} and n_{in} remain constant, while a and ϕ decrease since a decrease in cell radius a leads to a decrease in cell volume and thus in cell volume fraction ϕ. Figure 3(a) shows that if the cell radius is the only variable, μ_s' increases in response to cell shrinkage and decreases in response to cell swelling. In this case, $2\pi a n_{ex}/\lambda = 111$ is much larger than 50, so the Mie approximation might not be very accurate for predicting μ_s' values of the liver. However, the previous study[14] shows that the deviation of the Mie theory approximation, Eq. (1), from the exact Mie calculation is negligible when $(2\pi a n_{ex}/\lambda)$ increases from 5 to 100 with $n_{in}/n_{ex} = 1.05$. Following this
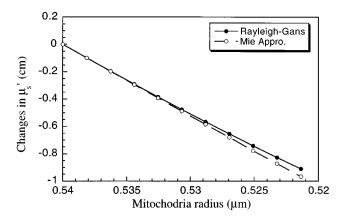
Fig. 4 A set of simulation results using the Rayleigh-Gans approximation to calculate changes in reduced scattering coefficient, μ_s', as a function of glucose concentration in the perfused liver. Three kinds of lines show the dependence of μ_s' on extracellular refractive index only (solid line), on both extracellular refractive index and cell size (long dashed line), and on extra- and intra-cellular refractive indexes and cell size (short dashed line). This figure shows that if n_{in} does not change, the effect of change in n_{ex} (giving a decrease of μ_s') is larger than that in cell size (giving an increase of μ_s'). Thus, the overall scattering will decrease. However, when n_{in} also varies, the effects of n_{in} and n_{ex} can compensate for one another, so the effect of changes in cell size becomes more significant.

Fig. 3 (a) Simulation results of the relationship between the reduced scattering coefficient, μ_s', and the cell radius for the perfused liver, based on both the Rayleigh-Gans (solid curve) and Mie theory (dashed curve) approximations. In this case, extra- and intracellular refractive indexes are fixed and equal to 1.33 and 1.38, respectively. (b) Simulation results of the dependence of μ_s' on both cell radius and extracellular refractive index, changed by adding glucose in the perfusate of the perfused liver. It is assumed that 500 mM glucose results in a 10% decrease in cell volume, and that the dependence of extracellular refractive index on glucose concentration [C] is given as $n(\text{out})=1.33+2.73\times10^{-5}[\text{C}]$ for a range of 0 to 500 mM.

trend, we estimate the error of the Mie approximation in Fig. 3(a) to be less than 5% with an n_{in}/n_{ex} ratio of 1.04.

When a solute such as glucose is added into the perfusate, two possible effects can occur in the perfused liver: a decrease in cell size due to a hyperosmotic pressure and an increase in extracellular refractive index. Both of these effects will change the overall scattering property of the liver. The results shown in Fig. 3(b) correspond to the calculations of μ_s' changes of a perfused rat liver as a function of cell radius (bottom scale) and of tissue extracellular refractive index (top scale). Both of these parameters change with an increase in glucose concentration in the perfusate. In the calculation, we varied the refractive index of the extracellular fluid as $n_{ex}=1.33+2.73\times10^{-5}\times[\text{C}]$ and assumed that 500 mM glucose results in a 10% decrease in cell volume, while keeping other parameters the same as those

used for Fig. 3(a), i.e., $a_0=10.68$ μm, $\phi_0=0.8$, $\lambda=800$ nm, and $n_{in}=1.38$. Figure 3(b) shows that if the addition of glucose or a carbohydrate in tissue causes changes in cell size and in extracellular refractive index, μ_s' of the corresponding system decreases as the added glucose or carbohydrate concentration increases.

Using the Rayleigh-Gans approximation, we show in Fig. 4 the simulated dependence of μ_s' changes in a perfused rat liver on added glucose concentration in the perfusate with three variable conditions: changes in n_{ex} only, changes in both n_{ex} and cell size, and changes in extra- and intracellular refractive indexes as well as cell size. For the last situation, the relationship between n_{in} and the glucose concentration [C] is assumed to be similar to n_{ex} as $n_{in}=1.38+2.73\times10^{-5}\times[\text{C}]$. This calculation illustrates that the reduced scattering coefficient μ_s' of living tissue can increase or decrease upon exposure to hypertonic pressure, such as a solute or carbohydrate solution, depending on whether the cell membrane is permeable to that solute or carbohydrate so that the intracellular refractive index changes accordingly.

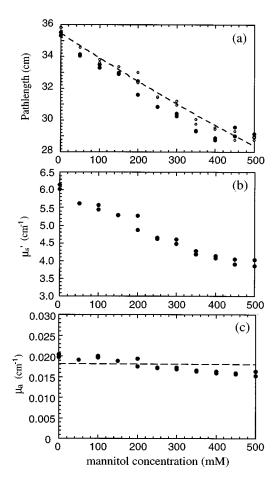### 4.1.3 Light Scattering by Mitochondria

It has been shown that an increase in cell volume induced by a hypo-osmotic imbalance leads to an increase in intramitochondrial volume.[24,25] In order to calculate the scattering effect at the mitochondrial scale using the two approximations, we think of a cell as a homogeneous medium with mitochon-

Fig. 5 Simulated dependence of changes in μ_s' on mitochondria radius of the rat liver. The only variable in this case is the mitochondria radius; other constant parameters used in the calculation are a_0=0.54 μm, ϕ_0=0.226, λ=0.8 μm, n_{ex}=1.38, n_{in}=1.42. The calculations were based on Eq. (3) along with Eqs. (1) and (2), respectively, for both the Mie theory approximation (open circles) and the Rayleigh-Gans approximation (solid circles).

dria distributed randomly inside as scatterers. The volume fraction of mitochondria in a liver cell is 22.6%, and its refractive index relative to the intracellular fluid is 1.04.[13] According to the same reference, we use the following parameters for mitochondria of the rat liver: a_0=0.54 μm, λ=0.8 μm, ϕ_0=0.226, n_{ex}=1.38, and n_{in}=1.42, which gives rise to $2\pi a n_{ex}/\lambda$=5.85. Thus, Eq. (3) is employed here with both approximations, Eqs. (1) and (2), in calculating changes in μ_s' as a function of mitochondrial radius, and the results are given in Fig. 5. It shows that (1) the deviation between the two approximations is very small, (2) μ_s' decreases as the radius of the mitochondria decreases. The latter behavior is in contrast to that in response to cell shrinkage, as shown in Fig. 3(a). The explanation may be that the factor of ϕ/a in Eq. (3) for mitochondria (ϕ=0.226) will decrease as the radius a and cell volume fraction ϕ, decrease since ϕ is on the order of a^3. However, the factor of $\phi(1-\phi)/a$ in Eq. (4) for liver cells (ϕ=0.8) will increase since $\phi(1-\phi)$ increases as ϕ decreases when ϕ>0.5. Therefore, it seems that a shrinkage in mitochondrial volume caused by hypertonic stress leads to only a decrease in overall scattering.

Thus, if an overall change in μ_s' results from both the cells and mitochondria, one will most likely obtain a decrease in μ_s' since the summation of the two calculated effects (shown in Figs. 4 and 5) gives a negative change. On the other hand, if changes in scattering in mitochondrial scales are negligible, one can have either an increase or a decrease in μ_s', depending on changes in cellular size and refractive indexes occurring at the cellular scale.

Fig. 6 Time-domain experimental results of a 0.5% Intralipid-mannitol suspension measured at 830 nm. This figure shows mean optical path length (a), reduced scattering coefficient μ_s' (b), and absorption coefficient μ_a (c) of the suspension as a function of mannitol concentration added in the suspension.

4.2 EXPERIMENTAL RESULTS OF SCATTERING CHANGES IN LIPID SUSPENSIONS AND THE PERFUSED LIVER

4.2.1 Changes in Light Scattering Caused by Solute Addition in Lipid Suspensions

Figure 6 plots a set of time-domain experimental results of a 0.5% Intralipid suspension as a function of mannitol concentration added into the suspension at a wavelength of 830 nm. By fitting the time-resolved spectroscopy data, we can obtain the values of mean optical path length, μ_s', and μ_a, as plotted in Figs. 6(a), 6(b), and 6(c), respectively. The solid data points in Fig. 6(a) were determined by substituting the measured reflectance into Eq. (5), whereas the dashed line with empty circles was calculated by replacing the fitted μ_a and μ_s' values in Eq. (6). The consistency between these two path length determinations demonstrates a good agreement between theory and experiment. Figures 6(a) and 6(b) clearly show that both the path length and the reduced scattering coefficient μ_s' decrease as the mannitol concentration added to the suspension in-

creases. Figure 6(c) shows a very small decrease in μ_a value while the mannitol concentration becomes larger (mean $\pm$S.D.$=0.018\pm0.002$ cm^{-1}). Very similar results have been obtained for glucose titration experiments (not shown).

4.2.2 Changes in Light Scattering Caused by Cell Swelling or Shrinkage in the Perfused Liver

In this section, we discuss changes in light scattering caused only by cell size variation in order to understand better the influence of cell size and cellular refractive indexes on light scattering with exposure of tissue to anisosmotic media. It has been reported that a decrease in liver temperature to 20 °C causes a net gain in cell K$^+$,[30] and that cooling mouse liver cells from 37 to 25 °C can lead to an increase in the membrane Na$^+$ to K$^+$ permeability ratio.[31] Both observations imply that with cooling, liver cells will have a net gain of Na$^+$ and K$^+$, so extracellular water may enter the cells in order to maintain osmotic balance. This water movement leads to cell swelling. It is also known that the temperature effect on the refractive index of a scattering fluid is relatively small,[7] thus changes in extracellular refractive index caused by temperature change can be ignored. Then, the overall μ_s' value or optical pathlength of the swollen cells of a cooled tissue should decrease according to the simulation in Fig. 3(a). In contrast, when the cooled tissue is warmed up, the cells will shrink and the μ_s' or path length will increase accordingly.

Temperature-dependent path length measurements were performed with the frequency-domain method (phase-modulation spectroscopy) on a perfused rat liver. In the experiment, the temperature of the liver was altered by changing the temperature of the perfusate, which was contained in a thermally controlled bath. Figure 7(a) corresponds to a cooling process of the liver from 37 °C, the perfusate temperature measured in the bath, to 25 °C in about 10 min. A few ($\sim$2.5) minutes after the perfusate started to cool down, the liver started to respond, and the path length kept decreasing as the liver temperature went down until the perfusate temperature stabilized at the setting temperature of 25 °C. In contrast, Fig. 7(b) shows an increase in path length when the perfusate of the perfused liver warmed up from 25 to 37 °C. The time courses for the cooling down [Fig. 7(a)] and warming up [Fig. 7(b)] processes are not necessarily the same, mainly depending on the amount of cooling source (ice) and heating power used. Figure 7 confirms the simulation results [Fig. 3(a)] that the scattering coefficient of the tissue, and thus corresponding optical path length measured, will increase or decrease with a decrease or increase in cell size.
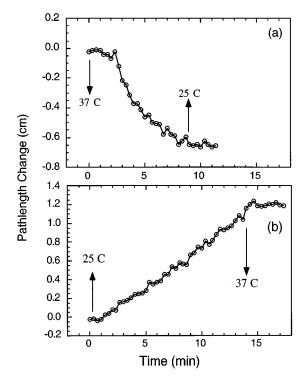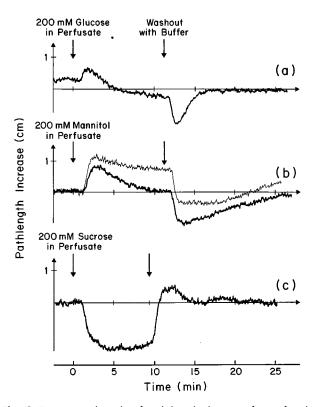

Fig. 7 Experimental results of temperature-dependent path length change in a perfused rat liver during a cooling (a) and warming-up (b) process. The data were obtained by the frequency-domain method.

4.2.3 Changes in Light Scattering Caused by Addition of Solute to the Perfused Liver

To study coupled effects on μ_s' due to changes in both cell size and refractive indexes of the tissue, we added several carbohydrates in the perfusate for the liver perfusion experiments. Figure 8 is a set of time-dependent curves of path length measurements using the frequency-domain method during liver perfusion with three kinds of carbohydrates. Curves (a), (b), and (c) correspond to a perfusate containing 200 mM glucose, 200 mM mannitol, and 200 mM sucrose, respectively. Two traces in curve (b) represent two measurements of two individual livers, demonstrating that different livers may be under different physiological conditions and thus have different response rates to mannitol. Figure 8 shows clearly that the path lengths or the scattering properties are different in these three cases. The similarity between the glucose and mannitol perfusion is that the path length increases as the carbohydrate perfusion starts. However, the path length in the glucose perfusion returned to its baseline much faster than that in the mannitol perfusion. In contrast to these two perfusions, the path length decreased when the sucrose perfusate entered the liver and did not return to its baseline until the sucrose started to be washed out by the buffer. To quantify the values of μ_a and μ_s', the time-domain method at 830 nm was used for another sucrose perfusion with a concentration of 100 mM, and the
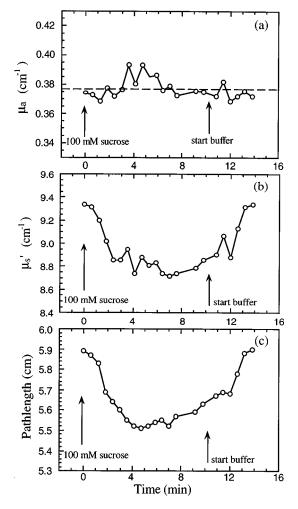
Fig. 8 Experimental results of path length changes of a perfused rat liver with (a) 200 mM glucose, (b) 200 mM mannitol, and (c) 200 mM sucrose, respectively, in the perfusate. The two traces in case (b) were obtained from two different rat livers.

Fig. 9 Experimental results of the absorption coefficient μ_a (a), the reduced scattering coefficient μ_s' (b), and mean optical path length (c) of a rat liver perfused with 100 mM sucrose at 830 nm. The data were determined by time-resolved spectroscopy.

results are given in Fig. 9. It shows that the μ_s' values as well as optical path lengths of the liver decreased with a small variation of μ_a (mean±S.D. =0.377±0.007 cm^{-1}) during the perfusion. Good consistency between the results obtained with the time- and frequency-domain methods was also attained for glucose and mannitol measurements.

5 DISCUSSION

The data given in Figs. 6 and 9 show a negligible change of μ_a and a consistent increase or decrease between μ_s' and path length due to addition of a carbohydrate in the suspensions or tissue. These results are in good agreement with Eq. (8). Therefore, we can conclude that an increase or decrease in path length measured in tissue that is due to addition of a carbohydrate reflects an increase or decrease of its overall scattering property.

The simulation and experimental results in Sec. 4 demonstrate that the reduced scattering coefficient of tissue can be affected largely by the changes in refractive indexes of the extra- and intracellular fluid and in cell volume caused by osmotic stress due to the addition of carbohydrate to the tissue. However, in the Intralipid–yeast suspension shown in earlier studies,[7] it seems that the effect of yeast cell variation is not very notable since the result in that case is very similar to that of the pure lipid suspension. This can be explained by two factors:

(1) the cell volume fraction relative to the whole suspension volume is very small; (2) the yeast cells have polysaccharide walls, which are much more rigid than the regular membranes of tissue cells. Thus, the cell size and cell volume fraction of yeast cells would not change significantly from the osmotic pressure caused by the carbohydrate added to the suspension.

The addition of a solute or carbohydrate into tissue can cause both a decrease in cell volume and an increase in refractive index of the extracellular fluid. These two changes contradict each other in the overall scattering behavior of the tissue. The calculation shown in Fig. 3(b) suggests that the effect of an increase of extracellular refractive index is larger, giving an overall decrease in μ_s'. However, if the intracellular refractive index also increases when the added carbohydrate is permeable to the cells, the change of cell size becomes the major factor since the effects of intra- and extracellular refractive indexes cancel one another, as shown in Fig. 4. In this case, the overall path length will in-

crease upon the exposure of the tissue to the added carbohydrate. Specifically, in the liver glucose perfusion measurements represented by curve (a) in Fig. 8, the mean path length of the perfused liver increased rapidly and then returned to its original value within 2 to 3 min. This increase in path length indicates that: (1) glucose may enter the cells and result in increases of both n_{in} and n_{ex} so that the effect of changes in refractive indexes is relatively small, and (2) a decrease in cell size and in the cell volume fraction must occur in the beginning of the perfusion, leading to an increase in path length and μ_s', but soon the shrunken cells regain some of their original volumes. When the washout buffer is switched on, the path length starts to decrease since in this case the cells are under hypotonic condition so that they start to swell. Again, the path length returns to its baseline in 3 min when the cells recover their initial volumes. The data for mannitol perfusion shown by curve (b) in Fig. 8 are similar to those in the glucose perfusion except that the rate of return to the baseline is slower for mannitol than for glucose. This can be explained by the smaller permeability of the liver cells to mannitol than to glucose, so the uptake and recovery rate is slower for mannitol than for glucose.

In principle, neither the regulatory volume increase nor decrease of tissue cells can regain the initial cell volume completely. This means that the path lengths given in curves (a) and (b) of Fig. 8 should not completely return to their initial values. However, a change in refractive index of the extracellular fluid also occurs and compensates for the effect of the change in cell volume. Thus, the path length trace can stay above the baseline, return to the baseline, or go below the baseline, as demonstrated by the two traces in curve (b), after the initial prominent response, largely depending on tissue type and the permeability of the cells to the added solute or carbohydrate.

For the sucrose perfusion, the path length data given by curve (c) in Fig. 8 are quite different from the other two cases in two aspects: (1) the path length decreases when the perfusion starts, and (2) the path length does not tend to return to its baseline until the washout buffer is switched on. It is known that (1) cell shrinkage occurs when the rat liver is perfused with sucrose,[22] (2) the refractive index of sucrose is 1.34783,[32] which is very similar to that of glucose (1.3479) for 20 °C, 10% sugar solutions, and (3) the liver cell membrane is impermeable to sucrose.[22] The first two points indicate that the effects caused by changes in cell size and in extracellular refractive index in the sucrose and glucose perfusion of the liver should be very similar. A possible explanation for the opposite path length/scattering feature in the sucrose perfusion lies with the impermeability of the liver cell membrane to sucrose. In this case, if no sugar enters the cells, the intracellular refractive index, n_{in}, would not change much to compensate for the effect of an increase in

n_{ex}, and the μ_s'/path length will decrease, as predicted by the calculations given in Fig. 4. In addition, the impermeability of the liver cell membrane to sucrose may be also taken to explain the nonreturn feature since in this case, only water movement from the intracellular to extracellular compartments is involved, preventing the regulatory volume increase.

As predicted by the simulations given in Fig. 5, the overall μ_s' will decrease if any decrease in mitochondrial volume is involved as a result of cell shrinkage under hyperosmotic stress. The data obtained in the glucose and mannitol perfusion experiments suggest that the major source for changes in scattering property results mainly from variations of refractive indexes in the cellular scale and of cell sizes due to osmotic imbalance in tissue. Changes in scattering caused by changes in mitochondrial volume are small, even though mitochondria are a major source for tissue scattering. However, living tissues consist of various and complex components, and many factors are involved and need to be considered, so further studies would be helpful to confirm our explanations of the experimental findings.

Detection *in vivo* of changes in scattering property as a result of glucose intake by human subjects has been reported.[5] The measurements were performed on the thigh of the subjects, and the scattering factor started to decrease a few minutes after glucose ingestion, in contrast to our results obtained in the liver glucose perfusion. This inconsistency may be due to the fact that the glucose *in vivo* measurement, performed on the human thigh, may include a large portion of muscle and blood, whereas the liver perfusion measurement only involves pure liver cells. Since muscle cells are absolutely nonspherical and very different from the liver cells in shape and composition, muscle cells may response to glucose quite differently from the liver cells. Also, when blood is involved in the measurement, the coupling of the glucose uptake process by the red blood cells and muscle cells complicates the mechanism of changes in scattering property. Further studies are needed for better understanding.

This study shows the possibility of using NIR techniques for noninvasive physiological monitoring, such as monitoring tissue swelling by detecting path length (i.e., scattering property) changes. For example, if the path length increases, we know that the cells are shrinking. This study also shows that scattering changes in living tissue result not only from the extracellular refractive index but also from the intracellular refractive index and cell size upon exposure of the tissue to osmotic pressure. If additions of solutes or carbohydrates are involved, one may encounter multiple effects due to changes in cell size and in cellular refractive indexes. However, by using suitable carbohydrates, such as glucose or mannitol, the effects of changes in cell size of tissue can be made to dominate so that tissue

swelling can still be detectable by monitoring the path length change. Furthermore, the choice of the appropriate organ may optimize the path length changes since, for example, on the basis of these limited experiments, the liver itself would appear to be optimal for measuring the effect of solute changes in the body.

In summary, the theoretical and experimental results of this study show that addition of a solute or carbohydrate to tissue affects the size of tissue cells and the refractive indexes of the extra- and intracellular fluid, and thus affects the overall tissue scattering properties. In theory, we employed both the Rayleigh-Gans and Mie theory approximations to calculate the effects of osmolarity and cellular refractive indexes on the reduced scattering coefficient of tissues and used photon diffusion theory to associate the reduced scattering coefficient with the optical path length. We have experimentally demonstrated two NIR techniques capable of measuring the changes of optical properties due to the addition of a solute in tissue models and in perfused rat livers. The temperature-dependent path length measurements of the perfused liver confirm the dependence of tissue scattering on the tissue cell size. The liver results obtained with three kinds of carbohydrate perfusion display different scattering aspects and can be well explained by changes in cell size and in intra- and extracellular refractive indexes. This study demonstrates that the NIR technique has a significant potential for noninvasive, physiological monitoring.

REFERENCES

1. H. Liu, B. Chance, A. H. Hielscher, S. L. Jacques, and F. K. Tittel, ''Influence of blood vessels on the measurement of hemoglobin oxygenation as determined by time-resolved reflectance spectroscopy,'' *Med. Phys.* **22**(8), 1209–1217 (1995).

2. S. Fantini, M. A. Franceschini-Fantini, J. S. Maier, S. A. Walker, B. Barbieri, and E. Gratton, ''Frequency-domain multichannel optical detector for noninvasive tissue spectroscopy and oximetry,'' *Opt. Eng.* **34**, 32–42 (1995).

3. H. Liu, D. A. Boas, Y. Zhang, A. G. Yodh, and B. Chance, ''Determination of optical properties and blood oxygenation in tissue using continuous NIR light,'' *Phys. Med. Biol.* **40**, 1983–1993 (1995).

4. S. J. Matcher, P. Kirkpatrick, K. Nahid, M. Cope, and D. T. Delpy, ''Absolute quantification methods in tissue near infrared spectroscopy,'' *Proc. SPIE* **2389**, 486–495 (1995).

5. J. S. Maier, S. A. Walker, S. Fantini, M. A. Franceschini, and E. Gratton, ''Possible correlation between blood glucose concentration and the reduced scattering coefficient of tissues in the near infrared,'' *Opt. Lett.* **19**(24), 2062–2064 (1994).

6. M. Kohl, M. Cope, M. Essenpreis, and D. Böcker, ''Influence of glucose concentration on light scattering in tissue-simulating phantoms,'' *Opt. Lett.* **19**(24), 2170–2172 (1994).

7. B. Chance, H. Liu, T. Kitai, and Y. Zhang, ''Effects of solutes on optical properties of biological materials: Models, cells, and tissues,'' *Anal. Biochem.* **227**, 351–362 (1995).

8. D. Haussinger and F. Lang, ''Cell volume in the regulation of hepatic function: A mechanism for metabolism control,'' *Biochim. Biophys. Acta* **1071**, 331–350 (1991).

9. M. Mcmanus, J. Fischbarg, A. Sun, S. Hebert, and K. Strange, ''Laser light-scattering system for studying cell volume regulation and membrane transport processes,'' *Am. J. Physiol.* **265**(Cell Physiol. 34), C562–C570 (1993).

10. L. Reynolds, C. Johnson, and A. Ishimaru, ''Diffusive reflectance from a finite blood medium: The modelling of fiber optic catheters,'' *Appl. Opt.* **15**, 2059–2067 (1976).

11. J. M. Steinke and A. P. Shepherd, ''Comparison of Mie theory and the light scattering of red blood cells,'' *Appl. Opt.* **27**, 4027–4033 (1988).

12. B. Beauvoit, H. Liu, K. Kang, P. D. Kaplan, M. Miwa, and B. Chance, ''Characterization of absorption and scattering properties for various yeast strains by time-resolved spectroscopy,'' *Cell Biophys.* **23**, 91–109 (1994).

13. B. Beauvoit, T. Kitai, and B. Chance, ''Contribution of the mitochondrial compartment to the optical properties of the rat liver: A theoretical and practical approach,'' *Biophys. J.* **67**, 2501–2510 (1994).

14. R. Graaff, J. G. Aarnoudse, J. R. Zijp, P. M. A. Sloot, F. F. M. de Mul, J. Greve, and M. H. Koelink, ''Reduced light-scattering properties for mixtures of spherical particles: A simple approximation derived from Mie calculations,'' *Appl. Opt.* **31**(10), 1370–1376 (1992).

15. C. F. Bohren and D. R. Huffman, *Absorption and Scattering of Light by Small Particles,* Wiley, New York (1983).

16. A. Ishimaru, *Wave Propagation and Scattering in Random Media,* Academic Press, San Diego (1978).

17. E. M. Sevick, B. Chance, J. Leigh, S. Nioka, and M. Maris, ''Quantitation of time- and frequency-resolved optical spectra for the determination of tissue oxygenation,'' *Anal. Biochem.* **195**, 330–351 (1991).

18. S. R. Arridge, M. Cope, and D. T. Delpy, ''The theoretical basis for the determination of optical pathlength in tissue: Temporal and frequency analysis,'' *Phys. Med. Biol.* **37**, 1531–1560 (1992).

19. M. S. Patterson, B. Chance, and B. C. Wilson, ''Time resolved reflectance and transmittance for the noninvasive measurement of tissue optical properties,'' *Appl. Opt.* **28**, 2331–2336 (1989).

20. B. Beauvoit, T. Kitai, H. Liu, and B. Chance, ''Time-resolved spectroscopy of mitochondria, cells, and rat tissues under normal and pathological conditions,'' *Proc. SPIE* **2326**, 127–136 (1994).

21. T. Bakker-Grünwald, ''Potassium permeability and volume regulation in isolated rat hepatocytes,'' *Biochim. Biophys. Acta* **731**, 239–242 (1983).

22. P. Haddad, T. Thalhammer, and J. Graf, ''Effect of hypertonic stress on liver cell volume, bile flow, and volume-regulatory K$^+$ fluxes,'' *Am. J. Physiol.* **256**, G563–G569 (1989).

23. G. Alpini, R. A. Garrick, M. J. T. Jones, R. Nunes, and N. Tavoloni, ''Water and nonelectrolyte permeability of isolated rat hepatocytes,'' *Am. J. Physiol.* **251**, C872–C882 (1986).

24. P. Espie, B. Guerin, and M. Rigoulet, ''On isolated hepatocytes mitochondrial swelling induced in hypoosmotic medium does not affect the respiration rate,'' *Biochim. Biophys. Acta* **1230**, 139–146 (1995).

25. A. P. Halestrap, ''The regulation of the matrix volume of mammalian mitochondria in vivo and in vitro and its role in the control of mitochondrial metabolism,'' *Biochim. Biophys. Acta* **973**, 355–382 (1989).

26. J. B. Chappell and K. N. Haarhoff, *Biochemistry of Mitochondria*, E. C. Slater, Z. Kanaiga, and L. Wojtczak, eds., pp. 75–91, Academic Press, London and New York (1967).

27. H. Liu, M. Miwa, B. Beauvoit, N. G. Wang, and B. Chance, ''Characterization of absorption and scattering properties of small-volume biological samples using time-resolved spectroscopy,'' *Anal. Biochem.* **213**, 378–385 (1993).

28. C. Hallbrucker, S. vom Dahl, M. Ritter, F. Lang, and D. Häussinger, ''Effects of urea on K$^+$ fluxes and cell volume in perfused rat liver,'' *Pflügers Archiv: Eur. J. Physiol.* **428**, 552–560 (1994).

29. F. P. Bolin, L. E. Preuss, R. C. Taylor, and R. J. Ference, ''Refractive index of some mammalian tissues using a fiber optic cladding method,'' *Appl. Opt.* **28**(12), 2297–2303 (1989).

30. L. Lambotte, P. J. Kestens, and J. J. Haxhe, ''Effect of hypo-

thermia on potassium movements in isolated perfused organs,'' *Arch. Int. Physiol. Biochim.* **74**, 541–544 (1966).

31. R. Wondergem and L. B. Castillo, ''Effect of temperature on transmembrane potential of mouse liver cells,'' *Am. J.* *Physiol.* **251**(Cell Physiol. 20), C603–C613 (1986).

32. M. Windholz, S. Budavari, R. F. Blumetti, and E. S. Otterbein, eds., *The Merck Index: An Encyclopedia of Chemicals, Drugs, and Biologicals,* Merck & Co., Rahway, NJ (1983).